Available online at www.sciencedirect.com

ScienceDirect

Energy Procedia 40 (2013) 285 – 293

Energy Procedia

European Geosciences Union General Assembly 2013, EGU

Division Energy, Resources & the Environment, ERE

Investigation of CO_2 release pressures in pipeline cracks

Paul Gorenz*, Nicoleta Herzog, Christoph Egbers

Department of Aerodynamics and Fluid Mechanics, Brandenburg University of Technology Cottbus, Siemens-Halske-Ring 14, 03046 Cottbus, Germany

Abstract

The Carbon Capture and Storage technology can reduce the emissions of carbon dioxide. Within this technology CO_2 is segregated from facilities with high pollutant emissions, transported by pipelines and stored in underground geological formations. In this work release pressures in pipeline puncture failures were investigated. In most cases corrosion or obsolescence are the reasons for pipeline damages. CO_2 will then escape from the pipeline and disperse. There are some studies of CO_2 dispersions but with different assumptions concerning pipeline release pressures. In this work computational fluid dynamics simulations were done to reduce the uncertainties regarding the pressure in pipeline cracks.

© 2013 The Authors. Published by Elsevier Ltd. Open access under CC BY-NC-ND license.
Selection and peer-review under responsibility of the GFZ German Research Centre for Geosciences

Keywords: CFD; pressurised CO_2 pipeline transport; pipeline puncture failure; release pressure

1. Introduction

The reduction of CO_2 emissions into the atmosphere is a big challenge in the 21st century. One of the most promoted technologies to do so is the Carbon Capture and Storage technology (CCS). Within this process chain CO_2 is collected in facilities with high CO_2 emissions, i.e. power plants that burn fossil fuels. Hence common power plants must be upgraded to be able to segregate carbon dioxide. Up to now there are three possible procedures to segregate the carbon dioxide (e.g. oxy-fuel combustion, pre and post combustion capture). After segregation CO_2 is transported to subsurface storage locations by pipeline,

* Corresponding author. Tel.: +49-(0)355-69-4624; fax: +49-(0)355-69-4891.
E-mail address: Paul.Gorenz@tu-cottbus.de.

1876-6102 © 2013 The Authors. Published by Elsevier Ltd. Open access under CC BY-NC-ND license.
Selection and peer-review under responsibility of the GFZ German Research Centre for Geosciences
doi:10.1016/j.egypro.2013.08.033

truck, train and/or ship. In most cases saline formations and exhausted gas fields are used for the deposition of CO_2.

In general a long distance must be passed between the segregation and sequestration location. As CO_2 is at normal conditions in the gaseous phase state it must be set under high pressure to enter denser phase states to make the pipeline transport more efficient. Normally the carbon dioxide is set into the liquid or supercritical phase state by compressor stations, which compress the gas up to 15 MPa. The head loss caused by the pipeline flow makes booster stations along the pipeline necessary to keep the CO_2 in a dense phase state. Following the Final Report for IEA Greenhouse Gas Programme [1] CO_2 can be transported over 300 km without any booster station.

There are different accidental release scenarios of CO_2 which have different leakage probabilities and causes, e.g. CO_2 can escape during the segregation, compression, transportation and/or injection process. Molag and Dam [2] classified the processes during the release of CO_2 from pressurised broken pipelines. Additionally they described the physics and also presented modelling approaches for each process. A representation of these processes is visualised in Fig. 1 which was published by Koornneef et al. [3]. Based on Molag and Dam [2] the processes are:

- The depressurisation of the pipeline leading to a propagation of a pressure wave inside the pipeline and a two-phase pipe flow.
- Jet expansion and flashing in small distances from the leakage hole.
- Air entrainment caused by the free jet. This will result in a decreasing air temperature and so in condensation and freezing of the water present in the air.
- Solid particle rainout and the formation of a dry ice bank which then sublimates.
- Vapour cloud dispersion in regions where the momentum of the jet is fully vanished.

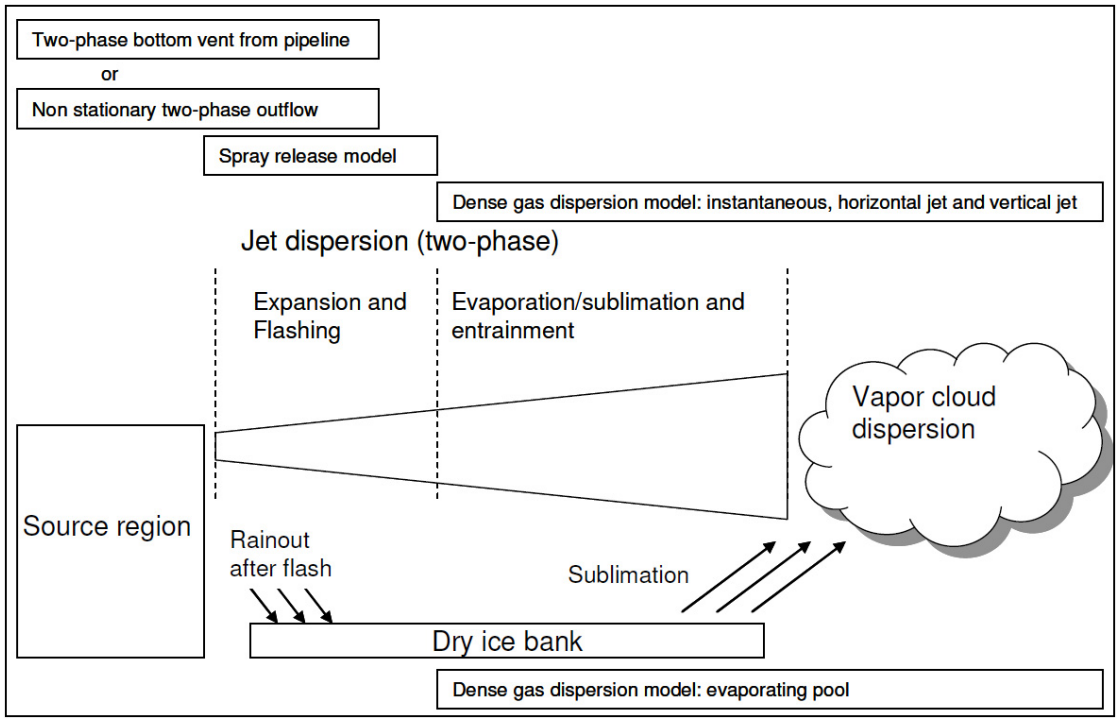

Fig. 1: Processes during the release of pressurised CO2 [3]

In principle leakages from pipelines may be classified into cases of a full rupture and a puncture failure each having a different CO_2 release and dispersion behaviour. These differences allow diverse approaches in the numerical modelling. For a full rupture Lund et al. [4] and Munkejord et al. [5] developed models that are capable to simulate the depressurisation of a CO_2 pipeline. The model of Lund is composed of a fluid dynamics part including the Euler equations for a single non-viscous fluid and a thermodynamics part with regard to the stiffened-gas equation of state. In both works one-dimensional simulations of a pipeline of $L = 100$ m with similar initial conditions were done. Wang et al. [6] investigated the simulation of variable-density turbulent axisymmetric jets which can develop from puncture leakages. Mazzoldi et al. investigated various aspects in the field of accidental CO_2 releases. A consideration of the jet-mixing effect is given in [7]. A model for the sublimation rate of CO_2 from a dry ice bank is presented in [8]. Furthermore Mazzoldi et al. compared CFD and Gaussian dispersion models in [9] and [10], whereas Herzog et al. [11] simulated the dispersion of a CO_2 cloud into the atmosphere. A review of several risk assessments for CO_2 transport pipelines is given by Koornneef et al. [3]. They discovered various uncertainties and knowledge gaps mostly concerning the dispersion behaviour and the appropriate modelling of it. Furthermore they noticed significant differences in the assumptions on pipeline diameter, pressure, temperature and sizes of leakage orifices.

This paper focuses on puncture failures of pressurised CO_2 pipelines and tries to reduce the uncertainties regarding the pressure in leakage orifices, which can be used for the dispersion calculation of CO_2 clouds. Within this work numerical simulations with the open source tool OpenFOAM were carried out to determine these release pressures. Therefore a 300 km pipeline between two booster stations was considered with the following assumptions:

- Pressure after a booster station: $p_{\text{booster station out}} = p_{\text{pipeline in}} = 14$ MPa
- Minimum allowed pressure in front of a booster station: $p_{\text{booster station in}} = p_{\text{pipeline out}} = 8$ MPa
- Constant temperature inside the pipeline: $T = 293$ K
- Transported fluid: liquid CO_2 (density $\rho = 900$ kg/m^3; kinematic viscosity $\nu = 8.9 \cdot 10^{-8}$ m^2/s)

These assumptions ensure that CO2 is transported in the liquid phase state. The pressure drop for laminar and turbulent pipeline flow is linear leading to a pressure drop of 20 Pa/m for the given assumptions.

According to Fig. 1 CO_2 is present in its liquid, gaseous and solid phase state during a release process. The scenario considered in this work focuses on the release pressure in the leakage hole and not on secondary effects occurring outside the puncture failure. Thus the processes inside the pipeline are decisive. Following Molag and Dam [2] there will be a two-phase outflow of liquid and vaporised CO_2 until the driving pressure difference has vanished. They also describe that at a certain point solid CO_2 will be formed when the pressure decreases below the CO_2 triple point pressure leading to much lower outflow rates. In this study the formation of dry ice is neglected because the assumptions and chosen boundary conditions ensure an operation above the CO_2 triple point. However, simulations were done for different pipeline diameters and leakage hole sizes. This makes the results of this study also applicable to scenarios in which clogging of the orifice due to the formation of dry ice is expected.

2. Computational setup and numerical method

The computational domain covers a 10 m pipeline segment around the leakage hole that take the following aspects into account: The simulation of a segment requires lesser cells than a full-pipeline mesh which results in a reduction of computation time. Furthermore it was assumed that the leakage hole has no significant influence on the pipeline flow in distances greater than 5 m from the orifice. Hence the leakage hole was chosen to be small in relation to the pipeline diameter. As the pressure in the pipeline

crack is of interest it was important for all outlet boundaries to have a certain distance to the leakage hole. Thus a cubic environment subdomain was additionally modelled around the leakage hole. This subdomain has a ten times larger edge length than the orifice dimensions, so it does not constrain the release behaviour of CO_2. The leakage hole itself is square formed. Simulations were done with the variation of the following parameters:

- Pipeline diameter: 0.5 m, 1.0 m and 1.5 m
- Leakage hole dimensions: 0.02 m × 0.02 m and 0.1 m × 0.1 m
- Leakage hole position at 10%, 50% and 90% of the 300 km pipeline in axial direction

For each position the head loss in this 10 m pipeline segment was set accordingly to the overall pressure loss of the 300 km pipeline which is in each case $\Delta p = 200$ Pa but with different pressure inlet and outlet boundary conditions as shown in Tab. 1. The boundaries of the environment subdomain were set to ambient conditions, i.e. total pressure of $p = 0.1$ MPa. For the velocity a no-slip condition was applied at the pipeline walls, whereas all other boundaries were set to *pressureInletOutletVelocity* which represents a zero gradient condition in normal direction of the boundary surface. In the initial state the pipeline was filled with liquid CO_2 and the subdomain contains air. Figure 2 shows the computational domain and the boundary conditions.

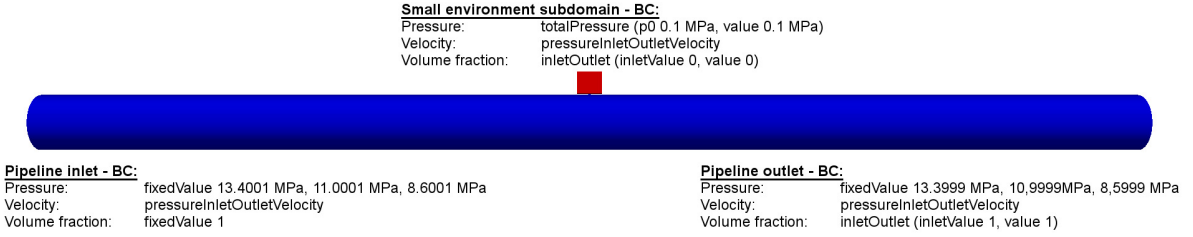

Fig. 2: Computational domain with boundary conditions

The mesh generation is done with a self-written Python-script which asks for the geometric properties of the domain, i.e. pipeline diameter, length ahead and after the leakage hole, the pipeline wall thickness and the dimensions of the orifice. In the leakage vicinity the mesh is finer than in the rest of the computational domain. The variation of the geometric properties (of pipeline diameter and leakage hole size) leads to a total of six meshes with different numbers of cells. The mesh with the least cells consists of $\approx 3 \cdot 10^5$ cells, whereas $\approx 8 \cdot 10^5$ cells were used for the mesh with the most cells.

Tab. 1: Pressure inlet and outlet boundary condition for the 10 m pipeline segments

Leakage hole position in axial pipeline direction [%]	Pressure at inlet [MPa]	Pressure at outlet [MPa]	Pressure loss per 10 m [Pa]
10	13.4001	13.3999	20
50	11.0001	10.9999	20
90	8.6001	8.5999	20

Due to the presence of liquid CO_2 and air inside the domain a two-phase solver with a volume of fluid approach (VOF) was utilised which is based on the work of Biausser et al. [12]. The original VOF method was introduced by Nichols and Hirt [13]. The governing equations are the conservation of mass:

$$\frac{\partial \rho}{\partial t} + \nabla \cdot (\rho \mathbf{u}) = 0 \tag{1}$$

and momentum:

$$\frac{\partial \rho \mathbf{u}}{\partial t} + \nabla \cdot (\rho \mathbf{u}\mathbf{u}) = -\nabla p - \nabla \cdot \left[\mu \left(\nabla \mathbf{u} + \nabla \mathbf{u}^T \right) \right] + \rho \mathbf{g} \tag{2}$$

for the phase mixture of CO_2 and air. Therein are **u** the velocity vector, p the pressure, t the time and **g** the gravity vector. As the code solves the governing equations for a single continuum (the phase mixture of liquid CO_2 and air) the density ρ and the dynamic viscosity μ in equations (1) and (2) must be variable across the domain. The local density and viscosity of the phase mixture can be computed by the following equations:

$$\rho = \alpha \rho_{liquid\,CO_2} + (1-\alpha)\rho_{air} \tag{3}$$

$$\mu = \alpha \mu_{liquid\,CO_2} + (1-\alpha)\mu_{air}, \tag{4}$$

where α is the volumetric phase fraction. The densities of the phases itself are constant leading to an incompressible treatment for each phase. Both phases are distinguished within a cell by the volume fraction α which is necessary to capture the interface between the phases. Due to the volume fraction the governing equations (1)-(2) are not closed. Thus an additional transport equation for α is required:

$$\frac{\partial \alpha}{\partial t} + \nabla \cdot (\alpha \mathbf{u}) = 0 \tag{5}$$

No mass transfer model is implemented in this code. Hence only mixing effects of liquid CO_2 and air can be simulated and no phase changes. For the computations Large Eddy Simulation (LES) was applied. For turbulence modelling sub-grid turbulent structures were modelled by the one equation LES model, whereas larger turbulent structures were resolved by the governing equations. The same code was validated and used by Herzog et al. [11].

3. Results

The calculated pressure values inside a leakage hole show a difference from the theoretical pressure which would be present in an unbroken pipeline. Fig. 4 shows the calculated release pressures for the different axial leakage hole positions on the pipeline. With the exception of the theoretical pressure curve the leakage hole release pressures are space and time averaged. Space averaging was done across the cross-section area of the orifice which is illustrated in red in Fig. 3. Time averaging was done over a time interval of 0.5 s. The coloured curves refer to the six meshes which result from the variation of the chosen pipeline diameters and leakage hole sizes.

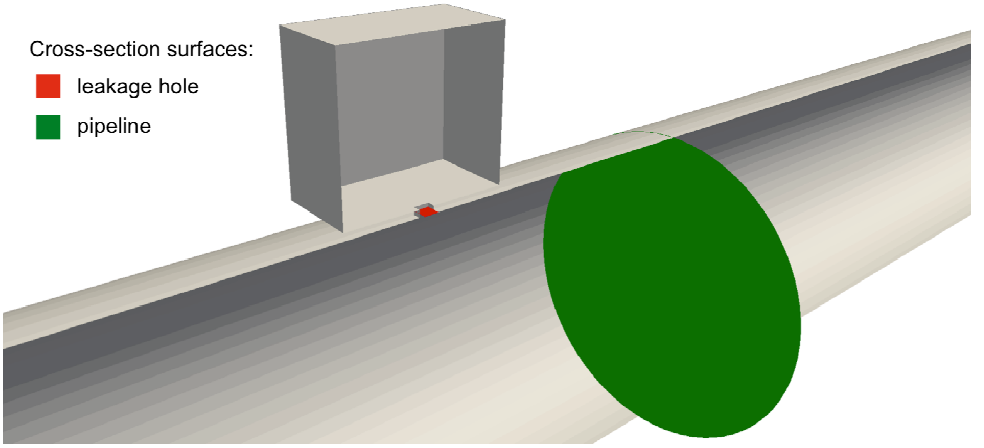

Fig. 3. Illustration of the cross-section surfaces used for the analysis

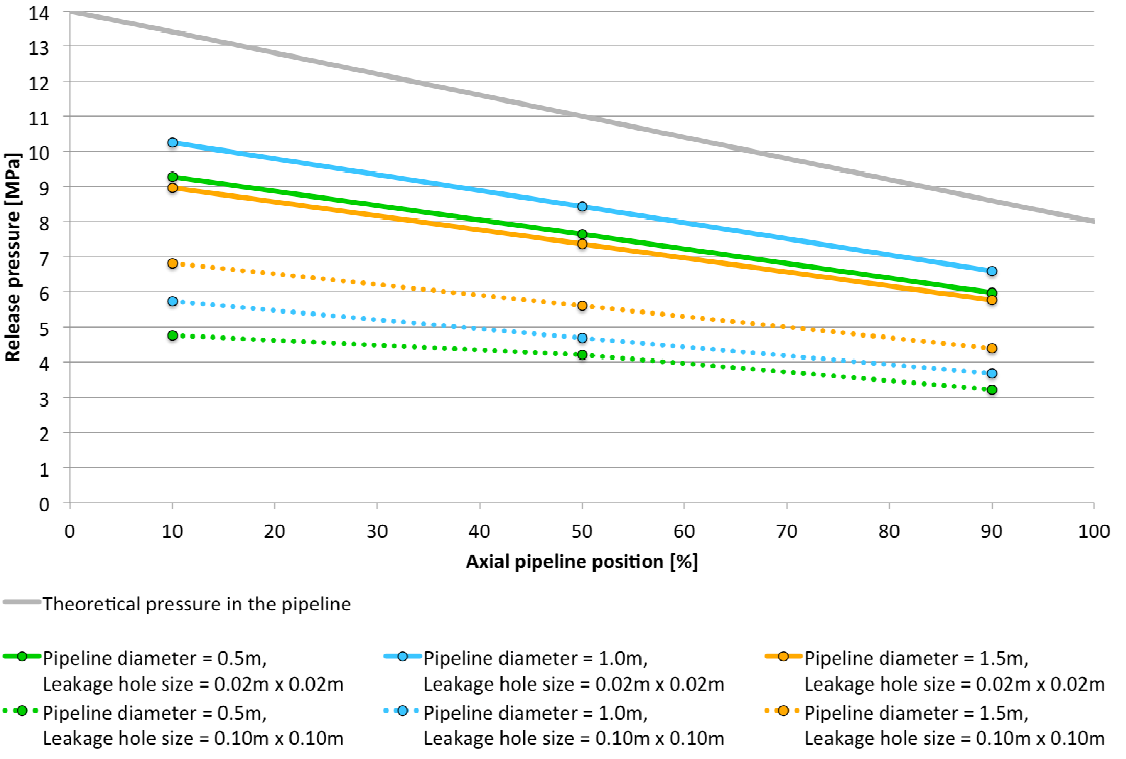

Fig. 4. Release pressures for different axial pipeline positions and geometric properties, i.e. pipeline diameter and leakage hole size

The comparison of the setups in Fig. 4 indicates lower release pressures for the cases with the larger leakage holes (0.1 m × 0.1 m). Thus the release pressure appears to be dependent on the ratio of the cross-section surfaces of pipeline and leakage hole:

$$\eta = \frac{A_{pipeline}}{A_{leakagehole}} \tag{6}$$

Therein is A the cross-section surface of the indexed variable which is shown in Fig. 3. The η values for the chosen cases are listed in Tab. 2.

Tab. 2: Cross-section surface ratios of pipeline to leakage hole

Leakage hole size [m²]	Pipeline diameter [m]	η [–]
0.1 × 0.1	0.5	19.63495408
0.1 × 0.1	1.0	78.53981634
0.1 × 0.1	1.5	176.7145868
0.02 × 0.02	0.5	490.8738521
0.02 × 0.02	1.0	1963.495408
0.02 × 0.02	1.5	4417.864669

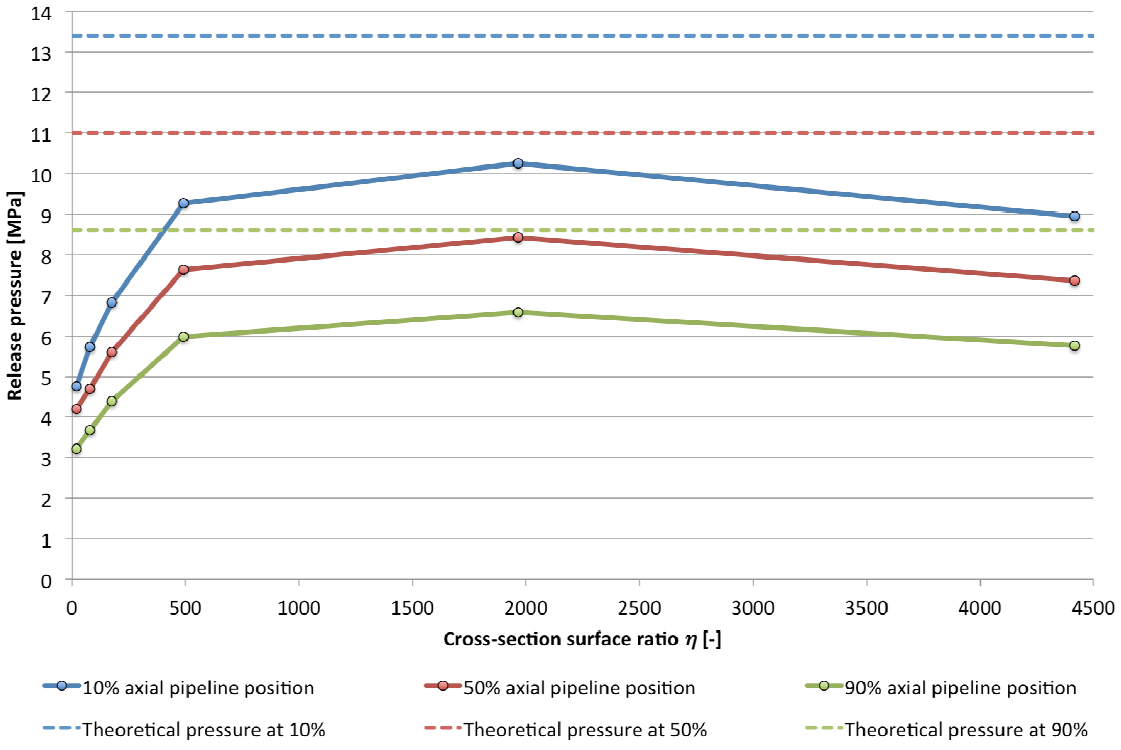

Fig. 5. Release pressures for the cross-section surface ratios of pipeline to leakage hole

Via η the results can be displayed in a chart that takes the ratio of the cross-section surfaces into account. Fig. 5 shows the release pressures depending on η for each setup and leakage hole position. Additionally the theoretical pressures of an unbroken pipeline for the given pipeline positions are displayed in this chart. For small η (≤ 500) an almost linearly dependency can be observed, whereas for $\eta > 500$ a nearly constant or a decreasing trend was calculated. This is expected because the release pressure cannot increase above the internal pipeline pressure (at a given position) for higher η.

4. Conclusion

Within this work the pressure inside pipeline cracks was investigated to reduce the uncertainties concerning an appropriate release pressure for CO_2 jet and cloud dispersion modelling. Therefore a 10 m pipeline as a segment of a 300 km pipeline between two booster stations was considered for numerical simulations. This pipeline segment had a puncture failure in the middle.

The results show a difference from the theoretical pressure values which would be present in an unbroken pipeline. Following Mazzoldi et al. [7] the leakage hole sizes considered in this work refer to medium and large leaks. In addition to this classification by Mazzoldi et al. the authors suggest to take the cross-section surface ratio of the pipeline (at the puncture failure) to the leakage hole into account. This allows a more general quantification for risk assessments because it can avoid the uncertainties regarding the pipeline diameters and failure sizes which are used for performing risk assessments. Koornneef et al. addressed these uncertainties in their work [3].

In this study a total of 18 cases were simulated by varying the pipeline diameter, leakage hole size and puncture failure position in axial direction on the pipeline. The results of these calculations were plotted in a chart which takes the cross-section surface ratio of pipeline to leakage hole into account. For a particular position higher release pressures were observed for an increasing cross-section surface ratio until this ratio reaches a value of $\eta \approx 500$. Higher ratios ($\eta > 500$) result in an almost constant trend of release pressures. This characteristic is expected because very high cross-section surface ratios imply pinhole leaks in relation to the pipeline. Thus the release pressure takes magnitudes of the pressure inside the pipeline.

Acknowledgements

This work was supported by the German Federal Ministry of Education and Research in the framework of the project GeoEn Verbundvorhaben GeoEnergie FKZ: 03 G 0767 B.

References

[1] Element Energy Limited. CO_2 pipeline Infrastructure: An analysis of global challenges and opportunities. *Final Report for International Energy Agency Greenhouse Gas Programme* 2010

[2] Molag M, Dam C. Modelling of accidental releases from a high pressure CO_2 pipelines. *Energy Procedia* 2011; **4**:2301-2307

[3] Koornneef J, Spruijt M, Molag M, Ramirez A, Faaij A, Turkenburg W. Uncertainties in risk assessment of CO_2 pipelines. *Energy Procedia* 2009; **1**:1587-1594

[4] Lund H, Flåtten T, Munkejord ST. Depressurization of carbon dioxide in pipelines – models and methods. *Energy Procedia* 2011; **4**:2984-2991

[5] Munkejord ST, Jakobsen JP, Austegard A, Mølnvik MJ. Thermo- and fluid-dynamical modelling of two-phase multi-component carbon dioxide mixture. *Int J Greenhouse Gas Control* 2010; **4**:589-596
[6] Wang P, Fröhlich J, Michelassi V, Rodi W. Large-eddy simulation of variable-density turbulent axisymmetric jets. *Int J Heat and Fluid Flow* 2008; **29**:654-664
[7] Mazzoldi A, Hill T, Colls J. A Consideration oft he jet-mixing effect when modelling CO_2 emissions from high pressure CO_2 transportation facilities. *Energy Procedia* 2009; **1**:1571-1578
[8] Mazzoldi A, Hill T, Colls J. CO_2 transportation for carbon capture and storage: Sublimation of carbon dioxide from a dry ice bank. *Int J Greenhouse Gas Control* 2008; **2**:210-218
[9] Mazzoldi A, Hill T, Colls J. CFD and Gaussian atmospheric dispersion models: A comparison for leak from carbon dioxide transportation and storage facilities. *Atmospheric Environ* 2008; **42**:8046-8054
[10] Mazzoldi A, Hill T, Colls J. Assessing the risk for CO_2 transport within CCS projects, CFD modelling. *Int J Greenhouse Gas Control* 2011; **5**:816-825
[11] Herzog N, Gorenz P, Egbers C. CFD modeling of high pressurized CO_2 released from onshore pipeline leakages. *Environ Earth Sci* 2012; DOI 10.1007/s12665-013-2536-3
[12] Biausser B, Grilli ST, Frauni´e P. Numerical simulations of three-dimensional wave breaking by coupling of a VOF method and a boundary element method. *Proc Annual Int Offshore and Polar Eng Conf* 2003; **3**:333-339
[13] Hirt CW, Nichols B. Volume of fluid method for the dynamics of free boundaries. *J Comp Physics* 1981; **39**:201-225